Potassium and Yttrium Complexes of a Rigid Bis-Phosphido POP-Donor Ligand

Kelly S. A. Motolko,[a] David J. H. Emslie,* [a] Hilary A. Jenkins[b] and James F. Britten[b]

Abstract: Dilithiation of 4,5-dibromo-2,7-di-*tert*-butyl-9,9-dimethylxanthene (XBr_2) followed by addition of 2 equiv. of (2,4,6-triisopropylphenyl)dichlorophosphine ($TrippPCl_2$) afforded 4,5-bis{(2,4,6-triisopropylphenyl)chlorophosphino}-2,7-di-*tert*-butyl-9,9-dimethylxanthene (XP_2Cl_2), which was reduced to 4,5-bis{(2,4,6-triisopropylphenyl)phosphino}-2,7-di-*tert*-butyl-9,9-dimethylxanthene (H_2XP_2) using excess $LiAlH_4$. Deprotonation of H_2XP_2 with excess KH in DME provided the dipotassium salt, $[K_2(XP_2)(dme)_n]$ (**1**; n = 2.5-4), and stirring **1** in THF followed by recrystallization from hexanes yielded tetrametallic $[K_4(XP_2)_2(THF)_4]$ (**2**) which features a central K_4P_4 cage. Reaction of $[YI_3(THF)_{3.5}]$ with $[K_2XP_2(dme)_{2.5}]$ afforded a mixture of products including $[(XP_2)YI(THF)_2]$ (**3**) and $(PTripp)_3$; pure **3** could be isolated in low yield by extraction with a minimum volume of hexanes or $O(SiMe_3)_2$. In the solid state, **3** adopts a face-capped trigonal bipyramidal coordination geometry with a planar xanthene backbone and an angle of 85° between the P(1)/C(4)/C(5)/P(2) and P(1)/Y/P(2) planes.

Introduction

Ancillary ligands play a critical role in defining the thermal stability and reactivity of metal complexes, and we have previously explored the use of rigid 4,5-bis(anilido)xanthene ligands in actinide and lanthanide chemistry. For example, the XA_2 {4,5-bis(2,6-diisopropylanilido)-2,7-di-*tert*-butyl-9,9-dimethylxanthene} pincer ligand was employed for the synthesis of thorium(IV), uranium(IV) and uranium(III) chloro complexes,[1,2] as well as dialkyl complexes of tetravalent thorium[1,3] and uranium[4] (Figure 1), thorium(IV) monoalkyl cations, and a thorium(IV) dication.[3,5] Furthermore, we recently reported the synthesis of Y, Lu and La derivatives of the XN_2 {4,5-bis(2,4,6-triisopropylanilido)-2,7-di-*tert*-butyl-9,9-dimethylxanthene} ligand, including monoalkyl derivatives (Figure 1) which are highly active catalysts for alkene and alkyne hydroamination.[6,7]

In combination with large rare earth and actinide elements, the xanthene-backbone XA_2 and XN_2 ligands present a rigid meridionally-coordinating pincer array that is capable of stabilizing highly reactive organometallic derivatives. Additionally, the rigidity of the ligand framework provides an opportunity to introduce softer donor atoms into the coordination sphere of rare earth or actinide elements, and we have previously prepared uranium(III) and (IV) complexes of a thioxanthene analogue of the XA_2 ligand, TXA_2.[2] As an extension of this concept, we became interested to probe the rare earth coordination behaviour of a 4,5-bis(arylphosphido)xanthene analogue of XN_2.

In comparison to amido ligands, phosphido ligands are far less explored in group 3 and f-element chemistry,[8] especially multidentate ligands containing phosphido donors. Ligands of this type which have been employed in rare earth chemistry are illustrated in Figure 2. The PN-, PO-, PPP-, OPO- and Cp/P-donor ligands a,[9,10,11] b,[9,12] c (L = PR_2),[13] c (L = OMe),[14] and f[15,16] were assembled prior to metal coordination. By contrast, d[11,17] and g[16] resulted from cyclometallation, and dianionic e[12] formed from monoanionic b (R' = H), via metal-mediated transfer of a methyl group from oxygen to the phosphorus donor of a second equivalent of ligand b.

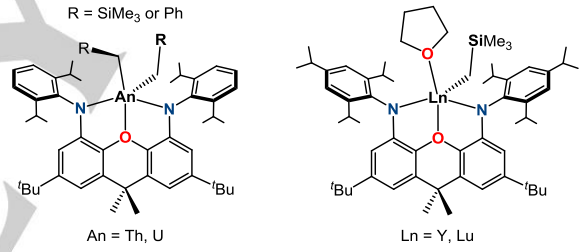

Figure 1. Neutral 4,5-Bis(anilido)xanthene Alkyl Complexes of thorium(IV), uranium(IV), yttrium(III) and lutetium(III).

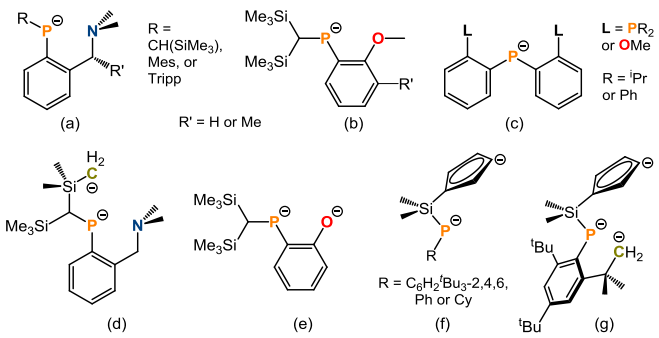

Figure 2. Multidentate phosphido ligands employed in rare earth chemistry.

Herein we report the synthesis of a direct phosphorus analogue of the $H_2[XN_2]$ pro-ligand, $H_2[XP_2]$, and potassium complexes of the XP_2 dianion, including the first example of a potassium phosphido compound with a K_4P_4 cubic cage structure. The synthesis and structural characterization of an yttrium iodido XP_2

[a] K. S. A. Motolko, Prof. D. J. H. Emslie
Department of Chemistry & Chemical Biology, McMaster University, 1280 Main St. West, Hamilton, Ontario, L8S 4M1 (Canada)
E-mail: emslied@mcmaster.ca
Web: http://www.chemistry.mcmaster.ca/emslie/emslie.html

[b] Dr. H. A. Jenkins, Dr. J. F. Britten
McMaster University Analytical X-Ray Diffraction Facility, 1280 Main St. West, Hamilton, Ontario, L8S 4M1 (Canada)

Supporting information for this article is given via a link at the end of the document.

complex is also described, allowing comparison of the binding preferences of XP_2 and XN_2 in the coordination sphere of yttrium.

Results and Discussion

Reaction of 4,5-dibromo-2,7-di-*tert*-butyl-9,9-dimethylxanthene (XBr_2) with 2 equiv of ^{n}BuLi in THF, followed by addition of 2 equiv of (2,4,6-triisopropylphenyl)dichlorophosphine (TrippPCl_2) afforded a 73 % yield of 4,5-bis{(2,4,6-triisopropylphenyl)-chlorophosphino}-2,7-di-*tert*-butyl-9,9-dimethylxanthene (XP_2Cl_2) as an approximate 1:1 ratio of diastereomers (Scheme 1; diastereomers were not assigned as *rac* or *meso* due to overlapping CMe_2 signals in ^{1}H and ^{13}C NMR spectra of the C_s-symmetric *meso* isomer). Samples enriched in each diastereomer could be obtained by washing the isolated solid with a small volume of hexanes; the solid residue contained > 95 % of one diastereomer, while the mother liquor contained > 60 % of the other diastereomer.

Pure or enriched samples of the diastereomers of XP_2Cl_2 were used to simplify NMR characterization. However, separation of diastereomers was not required prior to reaction with $LiAlH_4$ to form 4,5-bis{(2,4,6-triisopropylphenyl)phosphino}-2,7-di-*tert*-butyl-9,9-dimethyl-xanthene (H_2XP_2), which was isolated in 87 % yield as an approximate 1:1 mixture of diastereomers, containing 1.0-1.5 equiv of occluded LiCl based on elemental analysis (Scheme 1). The ^{1}H and ^{31}P NMR spectra of H_2XP_2 revealed $^1J_{1H,31P}$ couplings of 225 Hz and 229 Hz for the P-H signals of the two diastereomers, similar to those in Ph_2PH (218 Hz),[18] as well as related PCP-,[19] PNP-,[20] and POP-donor[21] pro-ligands (211-227 Hz).

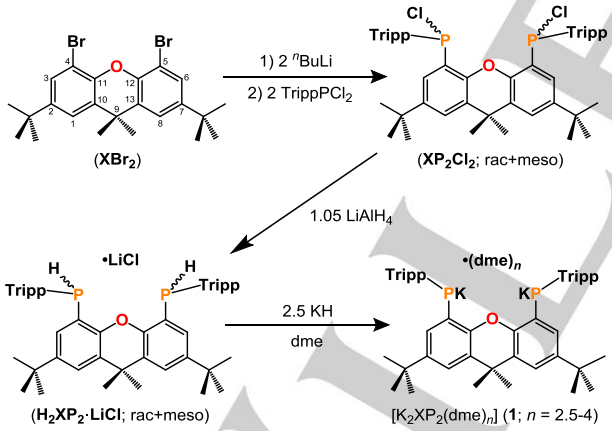

Scheme 1. Synthesis of XP_2Cl_2, H_2XP_2·LiCl and $[K_2(XP_2)(dme)_n]$ (n = 2.5-4). Tripp = 2,4,6-triisopropylphenyl.

Stirring H_2XP_2 with excess KH in DME for 72 h produced the dipotassium salt of the dianion, $[K_2(XP_2)(dme)_{2.5}]$ (**1**) as an orange solid in 80 % isolated yield (Scheme 1). The ^{31}P NMR spectrum of $[K_2(XP_2)(dme)_{2.5}]$ comprises of a single peak at –83.7 ppm, consistent with the removal of chirality at phosphorus upon deprotonation, and the ^{1}H NMR spectrum is indicative of C_{2v} symmetry. Crystals of $[K_2(XP_2)(dme)_4]$ were grown by cooling a concentrated DME solution to –30 °C (Figure 3) and reveal a K_2P_2 rhombus-shaped core, with 78-82° angles between the P(1)/C(4)/C(5)/P(2) and P(1)/K/P(2) planes. Two DME molecules are coordinated to each potassium atom and the ligand backbone is essentially planar with a 1° angle between the planes of the two aryl rings in the backbone.

Related phosphido complexes include polymeric $[\{K_2(POP)\}_\infty]$ {POP = 4,5-bis(*tert*-butylphosphido)-9,9-dimethyl-xanthene} featuring K···P and K···C_{aryl} contacts between adjacent K_2(POP) units,[21] $[\{(PNP)K_2(THF)_3\}_2]$ {PNP = 2,6-bis-(2-(phenylphosphido)phenyl)pyridine} with a ladder-like K_4P_4 core,[20] and polymeric $[\{(Ph_2P)K(pmdeta)\}_\infty]$, and $[\{(RPhP)K(pmdeta)\}_2]$ (R = $CH(SiMe_3)_2$; pmdeta = N,N,N',N'',N''-pentamethyldiethylene-triamine) with rhombus-shaped K_2P_2 cores.[22] The K–O_{xant} distances of 2.868(3) and 2.958(2) Å in **1** are similar to those in K_2(POP) {2.869(2) Å}, and the K–P distances in **1** {3.277(1) to 3.395(2) Å} fall within the range reported for the aforementioned literature compounds {3.128(1)-3.538(1) Å}. However, the C–P–C angles of 97.8(2) and 100.6(2)° are accute, more so than the compounds cited above {102.7(1)-107.5(1)°}, presumably to minimize unfavorable steric interactions between *ortho*-isopropyl groups and the two dme ligands on each potassium centre.

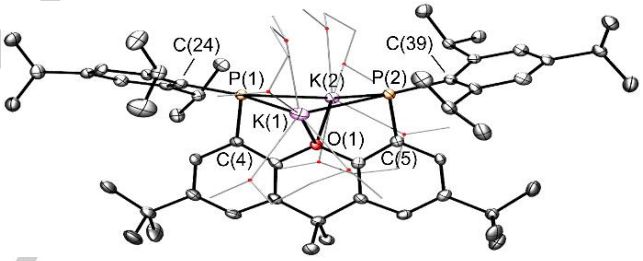

Figure 3. X-ray crystal structure of compound **1**. Ellipsoids are set at 50 % probability. The *tert*-butyl groups are rotationally disordered over multiple positions, and in each case, only one is shown for clarity. Hydrogen atoms are omitted, and the coordinating DME molecules are depicted in wire-frame. Selected bond lengths [Å] and angles [°]: K(1)–P(1) 3.395(2), K(1)–P(2) 3.332(1), K(2)–P(1) 3.320(1), K(2)–P(2) 3.277(1), K(1)–O(1) 2.868(3), K(2)–O(1) 2.958(2), P(1)–K(1)–P(2) 80.12(3), P(1)–K(2)–P(2) 82.03(3), K(1)–P(2)–K(2) 98.06(3), K(1)–P(1)–K(2) 96.00(3), C(4)–P(1)–C(24) 97.8(2), C(5)–P(2)–C(39) 100.6(2), K(1)-O(1)–K(2) 117.83(8), C(4)–P(1)–K(1) 84.2(1), C(4)–P(1)–K(2) 88.9(1), C(5)–P(2)–K(1) 85.5(1), C(5)–P(2)–K(2) 87.4(1), C(24)–P(1)–K(1) 134.1(1), C(24)–P(1)–K(2) 129.8(1), C(39)–P(2)–K(1) 130.2(1), C(39)–P(2)–K(2) 131.3(1).

Stirring $[K_2(XP_2)(dme)_{2.5}]$ (**1**) in THF at 24 °C for 5 h, followed by removal of the solvent *in vacuo* and recrystallization from hexanes afforded $[K_4(XP_2)_2(THF)_4]$ (**2**) as orange crystals in 22 % yield. The ^{1}H NMR spectrum of **2** contains a single complement of peaks for a top-bottom-symmetric XP_2 ligand (distinct from those of compound **1**), and the ^{31}P NMR spectrum features a single peak at –85.14 ppm, which is slightly shifted compared to that of **1**. The reaction to form **2** is reversible, since stirring **2** in DME at room temperature regenerates compound **1**.

The solid state structure of **2** consists of two $K_2(XP_2)$ units linked to form a K_4P_4 cube, with K–P–K and P–K–P angles of 80-

90° and 89-101°, respectively (Figure 4). The K–P distances in the square faces bridged by the xanthene backbone lie in a narrow range {3.201(3)-3.249(3) Å}, and are shorter than the K–P bonds in **1**. By contrast, the K–P distances linking these two faces are longer, at 3.328(3), 3.335(3), 3.540(3), and 3.568(3) Å; the two shorter K–P bonds are augmented by interactions between potassium and the *ipso*- and *ortho*-carbon atoms of an aryl group on phosphorus {K–C = 3.32(1)-3.40(1) Å; f in Figure 5}, whereas the longer K–P bonds are not bridged by comparable K–C_{aryl} interactions (K–C > 3.8 Å). Nevertheless, a similar range of K–P distances was reported for polymeric [{K_2(POP)}$_\infty$] {3.220(1)-3.518(1) Å}[21] and tetrametallic [{(PNP)K_2(THF)$_3$}$_2$] {3.228(1)-3.538(1) Å}.[20] The K–O_{THF} distances of 2.667(5)-2.712(6) Å in **2** lie within the typical range.[20,23] By contrast, the K–O_{xant} distances are significantly longer; at 3.033(6)-3.141(6) Å, these bonds are longer than the K–O_{xant} bonds in [K_2(XAT)(alkane)] {XAT = 4,5-bis(2,6-dimesitylanilido)-2,7-di-*tert*-butyl-9,9-dimethylxanthene; 2.534(3)-2.619(2)},[24] K_2(POP) {2.869(2) Å}, and **1** {2.868(3)-2.958(2) Å}.

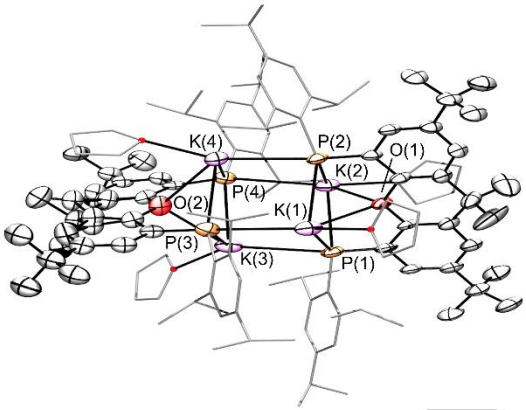

Figure 4. X-ray crystal structure of compound **2**. Ellipsoids are set at 50 % probability. Hydrogen atoms are omitted, and the 2,4,6-triisopropylphenyl groups and coordinated THF molecules are depicted in wire-frame. Interactions between K(1) and the aryl ring on P(3), and K(4) and the aryl ring on P(2) are not shown for clarity. The *tert*-butyl groups are rotationally disordered over multiple positions, and in each case, only one is shown for clarity. Selected bond lengths [Å] and angles [°]: K(1)–P(1) 3.203(3), K(1)–P(2) 3.218(3), K(2)–P(1) 3.201(3), K(2)–P(2) 3.232(3), K(3)–P(3) 3.249(3), K(3)–P(4) 3.217(3), K(4)–P(3) 3.221(3), K(4)–P(4) 3.215(2), K(1)–P(3) 3.328(3), K(2)–P(4) 3.540(3), K(3)–P(1) 3.568(3), K(4)–P(2) 3.335(3), K(1)–O(1) 3.141(6), K(2)–O(1) 3.049(5), K(3)–O(2) 3.033(6), K(4)–O(2) 3.127(5), K(3)–P(4)–K(2) 79.77(6), K(2)–P(1)–K(3) 79.56(6), all other K–P–K = 85.06(7)-90.37(6), P(1)–K(2)–P(4) 100.62(7), P(4)–K(3)–P(1) 99.71(7), all other P–K–P = 88.98(7)-95.66(7).

While a significant number of $Li_4(NR_2)_4$ cubic cage structures have been described,[25] only a handful of cubic $M_4(PnR_2)_4$ cage structures incorporating heavier alkali metal and/or pnictogen elements have been reported. In fact, structurally characterized examples are limited to [{Li_4(PH-Si^{t}BuAr-PSiPh$_3$)$_2$}$_2$(Li_2Cl_2)] featuring two Li_4P_4 cubes bridged by a Li_2Cl_2 unit (a in Figure 5);[26] [{Na_4(NMe$_2$)$_4$}{(Na(tmeda))$_3$(NMe$_2$)$_3$}$_2$] presenting a central Na_4N_4 cube linked via opposite faces to Na_3N_3 ladder structures; related [{Na_6(NMe$_2$)$_6$}{(Na(tmeda))$_3$(NMe$_2$)$_3$}$_2$] with an Na_6N_6 core composed of two face-sharing cubes (b in Figure 5); [{Rb(PH(Dmp))}$_4$]·C_7H_8 (Dmp = 2,6-dimesitylphenyl) with a Rb_4P_4 core (c in Figure 5);[27] [Cs_4{NH(SiMe$_3$)}$_4$] with a Cs_4N_4 core (d in Figure 5);[28] and [{Cs(η^6-Toluene)}$_4${P(H)Si^{t}Bu$_3$}$_4$] with a Cs_4P_4 core (e in Figure 5).[29] Compound **2** is therefore the first structurally characterized phosphido complex featuring a cubic K_4P_4 core.

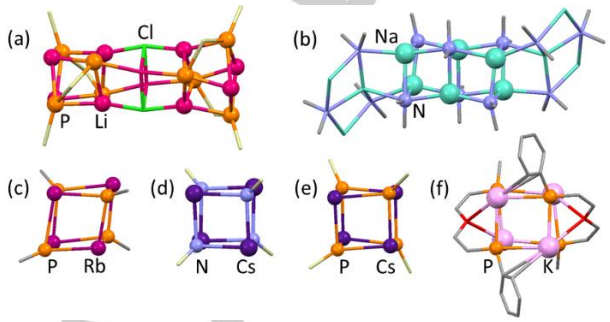

Figure 5. The central cores of (a) [{Li_4(PH-Si^{t}BuAr-PSiPh$_3$)$_2$}$_2$(Li_2Cl_2)], (b) [{Na_6(NMe$_2$)$_6$}{(Na(tmeda))$_3$(NMe$_2$)$_3$}$_2$], (c) [{Rb(PH(Dmp))}$_4$]·C_7H_8 (Dmp = 2,6-dimesitylphenyl), (d) [Cs_4{NH(SiMe$_3$)}$_4$], (e) [{Cs(η^6-Toluene)}$_4${P(H)Si^{t}Bu$_3$}$_4$], and (f) compound **2**. M_4Pn_4 cores are shown in ball-and-stick format, while key surrounding atoms (not including H atoms) are shown as capped sticks.

Reaction of [K_2(XP_2)(dme)$_{2.5}$] with [YI_3(THF)$_{3.5}$] in THF produced a mixture of products (consistently >10 peaks in the ^{31}P NMR spectrum) including [(XP_2)YI(THF)$_2$] (**3**) and tris(2,4,6-triisopropylphenyl)triphosphirane {(PTripp)$_3$};[30] the latter compound was identified by ^{1}H, ^{13}C and ^{31}P NMR spectroscopy (comparison with an independently prepared sample) and X-ray crystallography [Figure 6; the structure is closely analogous to those of (PMes)$_3$[31] and (PAnt)$_2$(PAr);[32] Mes = mesityl, Ant = 9-Anthracenyl; Ar = C_6H_2{*o*-CH(SiMe$_3$)$_2$}$_2${*p*-C(SiMe$_3$)$_3$}]. Crude **3** was isolated as the major product after extraction into a small volume of hexanes, and pure **3** was isolated as an orange powder via a second extraction with a small volume of either O(SiMe$_3$)$_2$ or hexanes in an 18 % overall yield (Scheme 2). X-ray quality crystals were obtained by cooling a concentrated hexanes solution of **3** to –30 °C (Figure 7). It is of note that the unexpected byproducts formed in the synthesis of **3** do not arise from thermal decomposition of **3** over the duration of the reaction, given that the ^{31}P NMR signal for **3** did not decrease in intensity once the reaction reached completion.

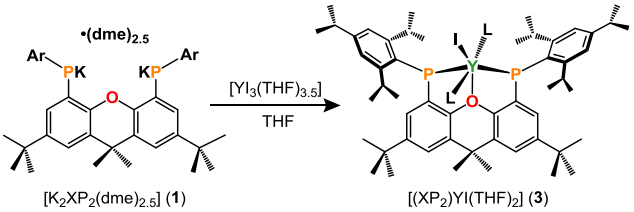

Scheme 2. Attachment of the XP_2 ligand to yttrium by salt metathesis (L = THF).

The X-ray crystal structure of **3** (Figure 7) revealed that the xanthene backbone of the XP_2 ligand is planar, and the geometry

at yttrium is approximately face-capped trigonal bipyramidal with the anionic donors in equatorial positions and the THF ligands in axial positions. Yttrium lies 1.55 Å out of the P(1)/C(4)/C(5)/P(2) plane, leading to an 85° angle between the P(1)/C(4)/C(5)/P(2) plane and the PYP plane. By comparison; yttrium lies 0.50 Å out of the N(1)/C(4)/C(5)/N(2) plane of the related XN_2 ligand in $[(XN_2)Y(CH_2SiMe_3)(THF)]$ (Figure 8), with a 31° angle between the N(1)/C(4)/C(5)/N(2) plane and the NYN plane.[6] The P(1)–Y–P(2), P(1)–Y–I, and P(2)–Y–I angles in the equatorial plane of **3** are 110.87(7), 122.43(5) and 121.79(5)°, respectively, with an I–Y–{P(1)P(2)centroid} angle of 159.5°. The O(2)–Y–O(3) angle is 162.0(2)°, and the O(2)–Y–I and O(3)–Y–I angles are 81.6(1)° and 81.9(1)°, respectively. The O(1) donor of the xanthene backbone caps the centre of the P(1)/P(2)/O(3) face with O(1)–Y–P and O(1)–Y–O(3) angles between 67.4(1) and 70.3(2)°.

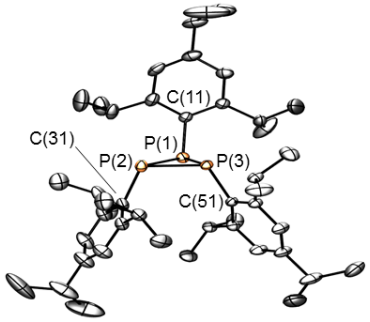

Figure 6. X-ray crystal structure of $(PTripp)_3$ with ellipsoids set to 50 % probability. Hydrogen atoms are omitted for clarity. Selected bond lengths [Å] and angles [°]: P(1)–P(2) 2.2367(6), P(1)–P(3) 2.2060(6), P(2)–P(3) 2.2151(6), P(1)–C(11) 1.864(2), P(2)–C(31) 1.852(2), P(3)–C(51) 1.849(2), P(2)–P(1)–P(3) 59.81(2), P(1)–P(2)–P(3) 59.41(2), P(1)–P(3)–P(2) 60.78(2), C(11)–P(1)–P(2) 101.01(5), C(11)–P(1)–P(3) 96.76(5), C(31)–P(2)–P(1) 107.69(6), C(31)–P(2)–P(3) 112.08(6), C(51)–P(3)–P(1) 115.24(5), C(51)–P(3)–P(2) 116.53(5).

The Y–P distances in **3** are 2.715(2) Å and 2.762(2) Å, falling near the middle of the spectrum observed for the terminal phosphido ligands in $[(Y\{P(SiMe_3)_2\}_2\{\mu\text{-}P(SiMe_3)_2\})_2]$ {2.660(2)-2.693(2) Å},[33] $[Y\{P(SiMe_3)Ar\}I_2(thf)_3]$ (Ar = 2,6-$C_6H_3{}^iPr_2$) {2.699(2) Å},[34] $[(Cp^{TMS2})_2Y(PHR)(THF)]$ {Cp^{TMS2} = 1,3-$C_5H_3(SiMe_3)_2$; R = Si^tBu_3) {2.770(1) Å},[33] $[\{(Me_4C_5\text{-}SiMe_2\text{-}PAr)Y(THF)(\mu\text{-}H)\}_2]$ (Ar = 2,4,6-$C_6H_2{}^tBu_3$) {2.724(1) Å}, $[\{Me_4C_5\text{-}SiMe_2\text{-}P\text{-}C_6H_2(2,4\text{-}{}^tBu)_2(6\text{-}CMe_2CH_2)\}Y(THF)_2]$ {2.789(2) Å}, $[\{(Me_4C_5\text{-}SiMe_2\text{-}PPh)Y(THF)(\mu\text{-}H)_2(\mu\text{-}PhP\text{-}SiMe_2\text{-}C_5Me_4)Y(THF)_2]$ {2.826(2) Å},[16] and $[(\kappa^3\text{-}Tp^*)(Cp)Y(PPh_2)(THF)]$ (Tp* = tris(3,5-dimethylpyrazolyl)-hydroborate) {2.845(2) Å}.[35]

The Y–I distance of 2.964(1) Å in **3** is also within the range previously reported for yttrium iodido compounds. For example, the Y–I distances are 2.9287(3) and 2.9464(3) Å in $[\{HC(CMeNAr)_2\}YI_2(THF)]$,[36] 2.947(1)-2.979(1) Å in $[Y\{P(SiMe_3)Ar\}I_2(thf)_3]$ (Ar = 2,6-$C_6H_3{}^iPr_2$),[34] and 3.0161(8) Å in $[YI\{N(SiMe_3)_2\}_2(CH_2PPh_3)]$.[37] The Y–$O_{THF}$ distances of 2.322(5) and 2.336(5) Å are typical,[36,38] whereas the Y–O(1) distance of 2.508(4) Å is substantially elongated, reflecting the poor donor ability of a diarylether ligand, combined with steric constraints imposed by the rigidity of the XP_2 pincer ligand framework.

Between 25 °C and –90 °C, solution ^{1}H NMR spectra of **3** in d_8-THF indicate apparent C_{2v} symmetry, consistent with rapid migration of the $YI(THF)_2$ unit from one side of the plane of the ligand backbone to the other. Compound **3** gave rise to a ^{31}P NMR signal at 1.28 ppm with a $^1J_{31P,89Y}$ coupling of 162 Hz. This coupling is slightly larger than those observed for the terminal yttrium phosphido complexes $[Y\{P(SiMe_3)Ar\}I_2(thf)_3]$ (Ar = $C_6H_3{}^iPr_2$-2,6) (157 Hz),[34] $[(Cp^{TMS2})_2Y(PHR)(THF)]$ {Cp^{TMS2} = 1,3-$C_5H_3(SiMe_3)_2$; R = Si^tBu_3) (144 Hz)[33] and $[(Y\{P(SiMe_3)_2\}_2\{\mu\text{-}P(SiMe_3)_2\})_2]$ (122 Hz),[39] and significantly larger than those reported for the aforementioned intact and cyclometallated Me_4C_5-$SiMe_2$-PAr complexes (53-84 Hz).[16]

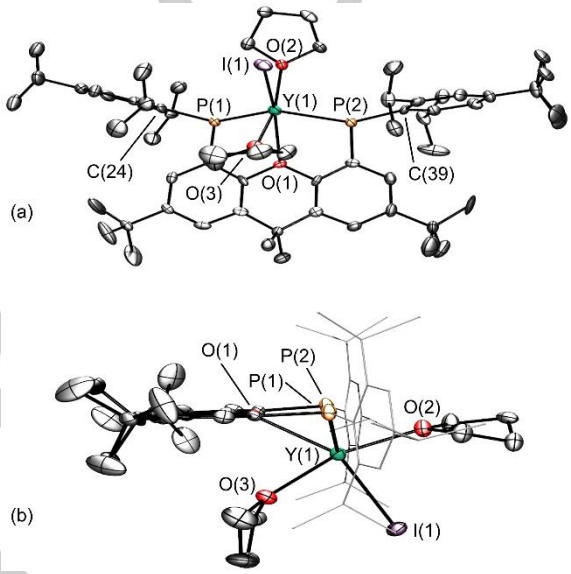

Figure 7. Two views of the X-ray crystal structure of compound **3**. Ellipsoids are set to 50 % probability. Hydrogen atoms are omitted for clarity. The *tert*-butyl groups are rotationally disordered over multiple positions, and in each case, only one is shown for clarity. In view b, the 2,4,6-triisopropylphenyl groups are depicted in wire-frame. Selected bond lengths [Å] and angles [°]: Y–P(1) 2.715(2), Y–P(2) 2.762(2), Y–I 2.9639(10), Y–O(1) 2.508(4), Y–O(2) 2.322(5), Y–O(3) 2.336(5), P(1)–Y–P(2) 110.87(7), P(1)–Y–I 122.43(5), P(2)–Y–I 121.79(5), O(2)–Y–O(3) 162.0(2), O(2)–Y–I 81.6(1), O(3)–Y–I 81.9(1), O(1)–Y–O(2) 126.6(2), O(1)–Y–O(3) 70.3(2), O(1)–Y–P(1) 68.6(1), O(1)–Y–P(2) 67.4(1).

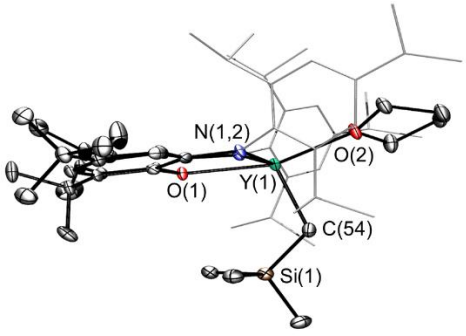

Figure 8. X-ray crystal structure of previously reported $[(XN_2)Y(CH_2SiMe_3)(THF)]$, highlighting the extent to which yttrium lies within the plane of the ligand. Reproduced with permission from reference 6. Copyright 2017 American Chemical Society.

In an attempt to isolate an XP_2 yttrium monoalkyl complex, two routes were employed; alkane elimination and salt metathesis. The alkane elimination reaction between $[Y(CH_2SiMe_3)_3(THF)_2]$ and H_2XP_2 (C_6D_6 solvent, 20 °C) yielded only unreacted H_2XP_2, and the products of $[Y(CH_2SiMe_3)_3(THF)_2]$ thermal decomposition. The salt metathesis reaction between **3** and $NaCH_2SiMe_3$ (1 or 2 equiv in THF) afforded a major product believed to be $[(XP_2)Y(CH_2SiMe_3)_2(THF)_n]^-$ by ^{1}H NMR spectroscopy. However, the reaction was not clean, and despite numerous attempts, this 'ate' complex could not be isolated in pure form.

Conclusions

The rigid POP pincer pro-ligand, H_2XP_2, was synthesized in two steps from XBr_2. Double deprotonation with excess KH yielded $[K_2XP_2(dme)_n]$ (**1**; n = 2.5-4) with a rhombus-shaped K_2P_2 core, or $[K_4(XP_2)_2(THF)_4]$ (**2**) featuring the first cubic K_4P_4 cage structure, depending on purification conditions. Reaction of **1** with $[YI_3(THF)_{3.5}]$ afforded $[(XP_2)YI(THF)_2]$ (**3**) in which Y is displaced 1.55 Å out of the P(1)/C(4)/C(5)/P(2) plane of the XP_2 ligand, contrasting the coordination behaviour of yttrium to XN_2, the amido-analogue of the XP_2 dianion. However, the reaction to form **3** is low yielding due to the formation of multiple products including tris(2,4,6-triisopropylphenyl)triphosphirane, $\{P(Tripp)\}_3$, indicative of poor ligand stability in the presence of strong Lewis acids.

Experimental Section

General Details: An argon-filled MBraun UNIlab glove box equipped with a –30 °C freezer was employed for the manipulation and storage of all air-sensitive compounds, and reactions were performed on a double manifold high vacuum line using standard techniques.[40] A Fisher Scientific Ultrasonic FS-30 bath was used to sonicate reaction mixtures where indicated. A VWR Clinical 200 Large Capacity Centrifuge (with 28° fixed-angle rotors that hold 12 × 15 mL or 6 × 50 mL tubes) in combination with 15 mL Kimble Chase glass centrifuge tubes was used when required (inside the glovebox). Residual oxygen and moisture was removed from the argon stream by passage through an Oxisorb-W scrubber from Matheson Gas Products. Diethyl ether, THF, toluene, benzene and hexanes were initially dried and distilled at atmospheric pressure from Na/Ph_2CO. Hexamethyldisiloxane ($O(SiMe_3)_2$) was dried and distilled at atmospheric pressure from Na. Unless otherwise noted, all proteo solvents were stored over an appropriate drying agent (pentane, hexanes, hexamethyldisiloxane ($O(TMS)_2$ / $O(SiMe_3)_2$) = Na/Ph_2CO/tetra-glyme; Et_2O = Na/Ph_2CO) and introduced to reactions via vacuum transfer with condensation at –78 °C. The deuterated solvents (ACP Chemicals) C_6D_6, THF-d_8 and toluene-d_8 were dried over Na/Ph_2CO.

The 4,5-Dibromo-2,7-di-*tert*-butyl-9,9-dimethylxanthene,[41] $[Y(CH_2SiMe_3)_3(THF)_2]$,[42] 2,4,6-triisopropylphenyldichlorophosphine,[43] and $NaCH_2SiMe_3$[44] starting materials were prepared according to literature procedures. 1,3,5-triisopropylbenzene, xanthone, KH (30 wt % in mineral oil), $LiCH_2SiMe_3$ (1.0 M in pentane), nBuLi (1.6 M in hexanes), Br_2, YI_3, YCl_3, NaO^{t}Bu and $LiAlH_4$ were purchased from Sigma-Aldrich. Solid $LiCH_2SiMe_3$ was obtained by removal of pentane *in vacuo*, and solid KH was obtained by filtration and washing with hexanes. $YI_3(THF)_{3.5}$ and $YCl_3(THF)_{3.5}$ were obtained by refluxing the anhydrous yttrium trihalide in THF for 24 h followed by removal of the solvent *in vacuo*. Argon (99.999 % purity) and ethylene (99.999 % purity) were purchased from Praxair.

Combustion elemental analyses were performed on a Thermo EA1112 CHNS/O analyzer at McMaster University and by Midwest Microlab, LLC, Indianapolis, Indiana. NMR spectroscopy (^{1}H, ^{13}C{^{1}H}, ^{31}P{^{1}H}, DEPT-Q, COSY, HSQC, HMBC) was performed on Bruker AV-200, DRX-500 and AV-600 spectrometers. All ^{1}H NMR and ^{13}C NMR spectra were referenced relative to $SiMe_4$ through a resonance of the employed deuterated solvent or proteo impurity of the solvent; C_6D_6 (7.16 ppm), d_8-Tol (2.08, 6.97, 7.01, 7.09 ppm), d_8-THF (1.72, 3.58 ppm) for ^{1}H NMR; and C_6D_6 (128.0 ppm), d_8-Tol (20.43, 125.13, 127.96, 128.87, 137.48 ppm), d_8-THF (25.31, 67.21 ppm) for ^{13}C NMR. ^{31}P{^{1}H} NMR spectra were referenced using an external standard of 85 % H_3PO_4 in D_2O (0.0 ppm). Herein, numbered proton and carbon atoms refer to the positions of the xanthene backbone, as shown in Scheme 1. Inequivalent ortho isopropyl protons are labeled A and B, so that the corresponding carbon resonances can be identified. X-ray crystallographic analyses were performed on suitable crystals coated in Paratone oil and mounted on a SMART APEX II diffractometer with a 3 kW Sealed tube Mo generator in the McMaster Analytical X-Ray (MAX) Diffraction Facility. In all cases, non-hydrogen atoms were refined anisotropically and H atoms were generated in ideal positions and then updated with each cycle of refinement. CCDC 1544974 (Compound **1**), 1544974 (Compound **2**), 1544974 (Compound **3**), and 1544977 {(PTripp)$_3$} contain the supplementary crystallographic data for this paper.

XP_2Cl_2: A 1.6 M solution of ^{n}BuLi in hexanes (12.3 mL, 19.6 mmol) was added to a solution of (4.72 g, 9.82 mmol) in THF (120 mL) at –78 °C, and the reaction mixture was stirred at –78 °C for 6 h. A solution of (6.0 g, 19.6 mmol) in THF (45 mL) was then added, and the reaction mixture and was allowed to warm to room temperature and stirred for 40 h. Solvent was removed *in vacuo* and the resulting yellow solid was dissolved in toluene (75 mL), centrifuged and the mother liquors were decanted and evaporated to dryness. To the resulting tacky yellow solid, hexanes (60 mL) was added followed by sonication and solvent removal *in vacuo* to yield XP_2Cl_2 as a free-flowing off-white solid (6.1 g, 73 %). This product is an approximate 1:1 mixture of diastereomers, and was of sufficient purity to proceed to the next step of the ligand synthesis (diastereomers were not identified as *rac* or *meso*, since both diastereomers gave rise to only one C*Me*$_2$ signal in the ^{1}H and ^{13}C NMR spectra, presumably due to overlapping signals in the case of the C_s-symmetric *meso* isomer). However, the diastereomers (referred to as A and B) could be separated by sonication in hexanes (4 mL per g of product) followed by centrifugation and separation of the solid from the mother liquors. The solid is > 95 % diastereomer A (isolated in 26 % yield from the crude) while the mother liquors are enriched in diastereomer B (a 3:1 B:A ratio is typical). ***NMR data for diastereomer A*: ^{1}H NMR (C_6D_6, 600 MHz):** δ 7.43, 7.15 (s, 2 × 2H, Xanth-C*H*^{1} and Xanth-C*H*^{3}), 7.23 (s, 4H, Ar-*H*), 4.25, 4.26 (sept, 2 × 2H, $^3J_{H,H}$ 6.5 Hz, ortho-C*H*Me$_2$), 2.76 (sept, 2H, $^3J_{H,H}$ 7.0 Hz, para-C*H*Me$_2$), 1.45 (s, 6H, C*Me*$_2$), 1.30, 1.26 (d, 2 × 12H, $^3J_{H,H}$ 6.5 Hz, ortho-CH*Me*$_2$), 1.20, 1.19 (d, 2 × 6H, $^3J_{H,H}$ 7.0 Hz, para-CH*Me*$_2$), 1.17 (s, 18H, C*Me*$_3$). **^{13}C NMR (C_6D_6, 126 MHz):** δ 156.40 (ortho-*C*CHMe$_2$), 152.54 (para-*C*CHMe$_2$), 150.56 (Xanth-*C*^{11}), 144.97 (Xanth-*C*^{2}), 130.64 (d, Ar-*C*$_{ipso}$), 129.83 (Xanth-*C*^{10}), 127.81, 125.85 (Xanth-*C*^{1}H and Xanth-*C*^{3}H), 122.94 (Ar-*C*H), 34.76 (para-*C*HMe$_2$), 33.42 (C*Me*$_2$), 32.31, 32.15 (2 × ortho-*C*HMe$_2$), 31.42 (C*Me*$_3$), 26.03, 24.40 (2 × ortho-CH*Me*$_2$), 24.02, 23.89 (2 × para-CH*Me*$_2$). **^{31}P NMR (C_6D_6, 243 MHz):** δ 75.52. ***NMR data for diastereomer B*: ^{1}H NMR (C_6D_6, 600 MHz):** δ 7.55, 7.41 (s, 2 × 2H, Xanth-C*H*^{1} and Xanth-C*H*^{3}), 7.24 (s, 4H, Ar-*H*), 4.31, 4.32 (sept, 2 × 2H, $^3J_{H,H}$ 6.7 Hz, ortho-C*H*Me$_2$), 2.78 (sept, 2H, $^3J_{H,H}$ 6.8 Hz, para-C*H*Me$_2$), 1.36 (s, 6H, C*Me*$_2$), 1.32, 1.27 (d, 2 × 12H, $^3J_{H,H}$ 6.7 Hz, ortho-CH*Me*$_2$), 1.24 (d, 12H, $^3J_{H,H}$ 6.8 Hz, para-CH*Me*$_2$), 1.13 (s, 18H, C*Me*$_3$). **^{13}C NMR (C_6D_6, 126 MHz):** δ 156.38 (ortho-*C*CHMe$_2$), 151.25 (Xanth-*C*^{11}), 149.15 (para-*C*CHMe$_2$), 147.46 (Xanth-*C*^{2}), 131.50 (Xanth-*C*^{10}), 130.62 (Ar-*C*$_{ipso}$), 127.83, 124.94 (Xanth-*C*^{1}H and Xanth-*C*^{3}H), 122.80 (Ar-CH), 34.73 (para-*C*HMe$_2$), 31.83, 31.60 (2 × ortho-*C*HMe$_2$), 31.70 (C*Me*$_2$), 31.49 (C*Me*$_3$), 25.62, 24.99 (2 × ortho-CH*Me*$_2$),

24.46, 24.40 (2 × para-CH*Me*$_2$). **^{31}P NMR (C_6D_6, 243 MHz):** δ 76.81. **Anal. Calcd. For $C_{53}H_{74}P_2OCl_2$:** C, 74.01; H, 8.67 %. Found: C, 73.85; H, 8.95 %.

H_2XP_2·*n*LiCl (*n* = 1–1.5): A solution of XP_2Cl_2 (4.0 g, 4.65 mmol) in toluene (60 mL) was added to a solution of $LiAlH_4$ (0.194 g, 5.11 mmol) in diethylether (200 mL) at –78 °C. The reaction mixture was stirred for 2 h before warming to room temperature and stirring for an additional 24 h. The solvent was removed *in vacuo* followed by centrifugation in toluene (45 mL) and evaporation of the mother liquor to dryness to yield a pale yellow solid. Hexanes (35 mL) was added followed by centrifugation and evaporation of the mother liquor. The resulting white solid was heated under vacuum at 60 °C for 2 days to remove all remaining solvent, yielding H_2XP_2·*n*LiCl (*n* = 1–1.5) (3.20 g, 87 %). **^{1}H NMR (C_6D_6, 600 MHz):** δ 7.34, 6.88 (m, 2 × 4H, Xanth-C*H*^{1} and Xanth-C*H*^{3} *rac* and *meso*), 7.27 (s, 8H, Ar-*H*, *rac* and *meso*), 6.37 (d, 2H, $^1J_{H,P}$ 229 Hz, P-*H*), 6.17 (d, 2H, $^1J_{H,P}$ 225 Hz, P-*H*), 4.01, 4.00 (2 sept, 2 × 4H, $^3J_{H,H}$ 6.5 Hz, ortho-C*H*Me$_2$ *rac* and *meso*), 2.83, 2.82 (2 sept, 2 × 2H, $^3J_{H,H}$ 7.0 Hz, para-C*H*Me$_2$ *rac* and *meso*), 1.54 (s, 6H, C*Me$_2$ rac*), 1.53, 1.51 (s, 2 × 3H, C*Me$_2$ meso*), 1.30, 1.27 (d, 2 × 12H, $^3J_{H,H}$ 6.5 Hz, ortho-CH*Me$_2$*), 1.25-1.23 (m, 48H, ortho- + para-CH*Me$_2$*), 1.17, 1.17 (s, 2 × 18H, C*Me$_3$ rac* and *meso*). **^{13}C NMR (C_6D_6, 126 MHz):** δ 155.43, (ortho-*C*CHMe$_2$), 151.12 (para-*C*CHMe$_2$), 149.71, 149.31 (Xanth-*C*^{11}), 145.98, 145.87 (Xanth-*C*^{2}), 129.36, 128.94 (Xanth-*C*^{10}), 127.81, 127.68 (Xanth-*C*^{1}H or Xanth-*C*^{3}H), 122.02, 121.87, 121.71 (Ar-*C*H + 2 × Xanth-*C*^{1}H or Xanth-*C*^{3}H), 35.26, 35.07, 34.67 (2 × Xanth-*C*^{9}Me$_2$ + *C*Me$_3$), 34.94 (para-*C*HMe$_2$), 33.49, 31.42 (C*Me$_2$ meso*), 33.39, 33.35, 33.31 (ortho-*C*HMe$_2$), 32.07 (C*Me$_2$ rac*), 31.63 (C*Me$_3$*), 25.43, 25.38 (ortho-CH*Me$_2$*), 24.45, 24.43, 24.25, 24.19 (ortho-CH*Me$_2$* + para-CH*Me$_2$*). **^{31}P NMR (C_6D_6, 81 MHz):** δ –93.07 d, ($^1J_{P,H}$ = 225 Hz), –93.77 d, ($^1J_{P,H}$ = 229 Hz). **Anal. Calcd. For $C_{53}H_{76}P_2O$:** C, 80.46; H, 9.68 %. Range from duplicate analyses on 4 different batches: C 76.49; H 9.72 % to C 74.78; H 8.70 %. These data correspond to ($C_{53}H_{76}P_2O$)·*n*LiCl (*n* = 1-1.5), since anal. calcd. for $C_{53}H_{76}P_2OLiCl$ is C 76.36; H 9.19 %, and anal. calcd. for $C_{53}H_{76}P_2OLi_{1.5}Cl_{1.5}$ is C 74.47; H 8.96 %.

[K_2(XP_2)(DME)$_{2.5}$] (1): Solid KH (0.126 g, 3.16 mmol) was added to a solution of H_2[XP_2]·*n*LiCl (*n*=1), (1.0 g, 1.20 mmol) in DME (40 mL), and the reaction was stirred at 24 °C for 72 h in the glove box. The orange reaction mixture was filtered, and the filtrate was evaporated to dryness *in vacuo*. Addition of hexanes (15 mL), centrifugation, and evaporation of the mother liquors to dryness afforded [K_2(XP_2)(DME)$_{2.5}$] (1.1 g, 80 %) as an orange solid. Crystals of [K_2(XP_2)(DME)$_4$] were grown by cooling a concentrated DME solution to –30 °C. **^{1}H NMR (C_6D_6, 600 MHz):** δ 7.43 (s, 4H, Ar-*H*), 6.78, 6.65 (s, 2H, Xanth-C*H*^{1} and Xanth-C*H*^{3}), 4.54 (sept, 4H, $^3J_{H,H}$ 6.5 Hz, ortho-C*H*Me$_2$), 3.06 (sept, 2H, $^3J_{H,H}$ 7.0 Hz, para-C*H*Me$_2$), 2.99 (s, 10H, 2.5 equiv. DME-CH$_2$), 2.88 (s, 15H, 2.5 equiv. DME-CH$_3$), 1.86 (s, 6H, C*Me$_2$*), 1.52 (d, 12H, $^3J_{H,H}$ 6.5 Hz, ortho-CH*Me$_2$*), 1.45 (d, 12H, $^3J_{H,H}$ 7.0 Hz, para-CH*Me$_2$*), 1.38 (d, 12H, $^3J_{H,H}$ 6.5 Hz, ortho-CH*Me$_2$*), 1.30 (s, 18H, C*Me$_3$*). **^{13}C NMR (C_6D_6, 126 MHz):** δ 155.16 (ortho-*C*CHMe$_2$), 146.78 (para-*C*CHMe$_2$), 144.70 (Xanth-*C*^{11}), 144.27 (Xanth-*C*^{2}), 141.18 (Ar-*C$_{ipso}$*), 126.34 (Xanth-*C*^{10}), 123.75, 110.69 (Xanth-*C*^{1}H and Xanth-*C*^{3}H), 120.69 (Ar-*C*H), 71.46 (DME-CH$_2$), 58.49 (DME-CH$_3$), 35.12 (para-*C*HMe$_2$), 34.61 (Xanth-*C*^{9}Me$_2$ and/or *C*Me$_3$), 34.16 (C*Me$_2$*), 33.73 (ortho-*C*HMe$_2$), 31.96 (C*Me$_3$*), 26.07, 25.00 (2 × ortho-CH*Me$_2$*), 24.72 (para-CH*Me$_2$*). **^{31}P NMR (C_6D_6, 81 MHz):** δ –83.73. **Anal. Calcd. For $C_{63}H_{99}P_2O_6K_2$:** C, 69.25; H, 9.13 %. Found: C, 69.69; H, 8.98 %.

[K_4(XP_2)$_2$(THF)$_4$] (2): [K_2(XP_2)(dme)$_{2.5}$] (**1**) (95 mg, 0.087 mmol) was dissolved in THF (12 mL) and stirred at 24 °C for 5 h, followed by removal of solvent *in vacuo*. The resulting amber colored solid was recrystallized from hexanes (1.5 mL) to yield [K_4(XP_2)$_2$(THF)$_4$] (38 mg, 21.6 %) as red-orange crystals. **^{1}H NMR (C_6D_6, 600 MHz):** δ 7.43 (s, 8H, Ar-*H*), 6.87 (d, 4H, $^4J_{H,H}$ 2.29 Hz, Xanth-C*H*^{1}), 6.61 (broad s, 4H, Xanth-C*H*^{3}), 4.37 (sept, 8H, $^3J_{H,H}$ 7.01 Hz, ortho-C*H*Me$_2$), 3.55 (m, 16H, 4 equiv. THF-C^{2,5}*H$_2$*), 3.07 (sept, 4H, $^3J_{H,H}$ 7.01 Hz, para-C*H*Me$_2$), 1.88 (s, 12H, C*Me$_2$*), 1.50 (d, 24H, $^3J_{H,H}$ 6.99 Hz, **A**-ortho-CH*Me$_2$*), 1.46 (d, 24H, $^3J_{H,H}$ 7.02 Hz, para-CH*Me$_2$*), 1.41 (m, 16H, 4 equiv. THF-C^{3,4}*H$_2$*), 1.34 (d, 24H, $^3J_{H,H}$ 6.99 Hz, **B**-ortho-CH*Me$_2$*), 1.33 (s, 36H, C*Me$_3$*). **^{13}C NMR (C_6D_6, 126 MHz):** δ 154.99 (ortho-*C*CHMe$_2$), 147.06 (para-*C*CHMe$_2$)), 144.57 (Xanth-*C*^{2}), 126.98 (Xanth-*C*^{10}), 124.07 (Xanth-*C*^{3}H), 120.80 (Ar-*C*H), 110.75 (Xanth-*C*^{1}H), 67.82 (THF-C^{2,5}H$_2$), 35.12 (para-*C*HMe$_2$), 34.83 (Xanth-*C*^{9}Me$_2$), 34.66 (*C*Me$_3$), 33.69 (ortho-*C*HMe$_2$), 33.54 (C*Me$_2$*), 31.95 (C*Me$_3$*), 25.94 (**B**-ortho-CH*Me$_2$*), 25.80 (THF-C^{3,4}H$_2$), 25.04 (**A**-ortho-CH*Me$_2$*), 24.69 (para-CH*Me$_2$*). **^{31}P NMR (C_6D_6, 81 MHz):** δ –85.14. **Anal. Calcd. For $C_{122}H_{180}O_6P_4K_4$:** C, 72.43; H, 8.97 %. Found: C, 72.38; H, 8.75 %.

[(XP_2)YI(THF)$_2$] (3) and ($PTripp$)$_3$: [K_2(XP_2)(dme)$_{2.5}$] (**1**) (0.250 g, 0.228 mmol) and [YI_3(THF)$_{3.5}$] (0.166 g, 0.228 mmol) were stirred in THF (25 mL) for 72 h at 24 °C. The bright yellow solution was filtered and the solvent was removed *in vacuo*. The resulting yellow solid was slurried in hexanes (8 mL) before the mixture was centrifuged and the mother liquors were evaporated to dryness to provided impure [(XP_2)YI(THF)$_2$] (**3**; 0.110 g) as an orange solid. 5 mL of O(SiMe_3)$_2$ was added to the impure solid followed by centrifugation. The resulting solid was isolated and dried *in vacuo* yielding pure [(XP_2)YI(THF)$_2$] (0.048 g, 18 % yield). The remaining mother liquors contain a mixture of products, including ($PTripp$)$_3$, and X-ray quality crystals of ($PTripp$)$_3$ were obtained by cooling a concentrated hexanes solution of this mixture to –30 °C. X-ray quality crystals of **3** were grown by cooling a concentrated hexanes solution of **3** to –30 °C. Solid samples of [(XP_2)YI(THF)$_2$] were observed to lose THF slowly under dynamic vacuum, and the sample used for NMR spectroscopic characterization contained just 1.5 equiv. of THF. **^{1}H NMR (d_8-THF, 600 MHz):** δ 7.11 (s, 4H, Ar-*H*), 6.74 (d, 2H, $^4J_{H,H}$ 2.0 Hz, Xanth-C*H*^{1}), 5.94 (dd, 2H, $^4J_{H,H}$ 2.0 Hz, $^3J_{P,H}$ 8.0 Hz, Xanth-C*H*^{3}), 4.40 (sept, 4H, $^3J_{H,H}$ 7.0 Hz, ortho-C*H*Me$_2$), 3.62 (m, 6H, 1.5 equiv. THF-C$^{2.5}$*H$_2$*), 2.92 (sept, 2H, $^3J_{H,H}$ 7.0 Hz, para-C*H*Me$_2$), 1.77 (m, 6H, 1.5 equiv. THF-C^{3,4}*H$_2$*), 1.54 (s, 6H, C*Me$_2$*), 1.28 (d, 12H, $^3J_{H,H}$ 7.0 Hz, para-CH*Me$_2$*), 1.24 (d, 12H, $^3J_{H,H}$ 7.0 Hz, **A**-ortho-CH*Me$_2$*), 1.01 (d, 12H, $^3J_{H,H}$ 7.0 Hz, **B**-ortho-CH*Me$_2$*), 0.99 (s, 18H, C*Me$_3$*). **^{13}C NMR (d_8-THF, 126 MHz):** δ 155.69 (ortho-*C*CHMe$_2$), 149.28 (para-*C*CHMe$_2$)), 144.06 (Xanth-*C*^{2}), 136.51 (d, Ar-*C$_{ipso}$*), 128.02 (Xanth-*C*^{10}), 123.94 (Xanth-*C*^{3}H), 121.66 (Ar-*C*H), 114.83 (Xanth-*C*^{1}H), 35.24 (para-*C*HMe$_2$), 34.66 (*C*Me$_3$), 34.53 (ortho-*C*HMe$_2$), 34.45 (Xanth-*C*^{9}Me$_2$), 33.11 (C*Me$_2$*), 31.49 (C*Me$_3$*), 26.18 (**B**-ortho-CH*Me$_2$*), 25.66 (**A**-ortho-CH*Me$_2$*), 24.34 (para-CH*Me$_2$*). **^{31}P NMR (d_8-THF, 81 MHz):** δ 1.28 (d, $^1J_{Y,P}$ = 162 Hz). **Anal. Calcd. For $C_{61}H_{90}P_2YIO_3$:** C, 63.76; H, 7.89 %. Found: C, 60.56; H, 7.95 %. (This compound is extremely air, moisture and temperature sensitive, and some decomposition may have occurred during transport to Indianapolis for elemental analysis).

Acknowledgements

D.J.H.E. thanks NSERC of Canada for a Discovery Grant and an NSERC Strategic Grant in collaboration with NOVA Chemicals. K.S.A.M. thanks the Government of Ontario for an OGS - Queen Elizabeth II Graduate Scholarship in Science and Technology (QEII GSST) scholarship. The authors would like to thank Dr. Hilary Jenkins and Dr. James F. Britten from the McMaster Analytical X-ray Diffraction Facility (MAX) for assistance with operation and analysis of single crystal x-ray diffraction.

Keywords: Cage compound • Phosphido ligand • Pincer ligand • Potassium • Yttrium

[1] C. A. Cruz, D. J. H. Emslie, L. E. Harrington, J. F. Britten, C. M. Robertson, *Organometallics* **2007**, *26*, 692-701.

[2] B. Vidjayacoumar, S. Ilango, M. J. Ray, T. Chu, K. B. Kolpin, N. R. Andreychuk, C. A. Cruz, D. J. H. Emslie, H. A. Jenkins, J. F. Britten, *Dalton Trans.* **2012**, *41*, 8175-8189.

[3] C. A. Cruz, D. J. H. Emslie, L. E. Harrington, J. F. Britten, *Organometallics* **2008**, *27*, 15-17.

[4] N. R. Andreychuk, S. Ilango, B. Vidjayacoumar, D. J. H. Emslie, H. A. Jenkins, Organometallics; *Organometallics* **2013**, *32*, 1466-1474.

[5] C. A. Cruz, D. J. H. Emslie, C. M. Robertson, L. E. Harrington, H. A. Jenkins, J. F. Britten, *Organometallics* **2009**, *28*, 1891-1899.

[6] K. S. A. Motolko, D. J. H. Emslie, H. A. Jenkins, *Organometallics* **2017**, *36*, 1601-1608.

[7] K. S. A. Motolko, D. J. H. Emslie, J. F. Britten, *RSC Advances* **2017**, *7*, *asap*.

[8] T. S. Li, S. Kaercher, P. W. Roesky, *Chem. Soc. Rev.* **2014**, *43*, 42-57.

[9] K. Izod, P. O'Shaughnessy, J. M. Sheffield, W. Clegg, S. T. Liddle, *Inorg. Chem.* **2000**, *39*, 4741-4748.

[10] (a) S. Blair, K. Izod, W. Clegg, *J. Organomet. Chem.* **2003**, *688*, 92-99; (b) K. Izod, S. T. Liddle, W. Clegg, R. W. Harrington, *Dalton Trans.* **2006**, 3431-3437.

[11] K. Izod, S. T. Liddle, W. McFarlane, W. Clegg, *Organometallics* **2004**, *23*, 2734-2743.

[12] W. Clegg, K. Izod, S. T. Liddle, P. O'Shaughnessy, J. M. Sheffield, *Organometallics* **2000**, *19*, 2090-2096.

[13] M. Mazzeo, M. Lamberti, I. D'Auria, S. Milione, J. C. Peters, C. Pellecchia, *J. Polym. Sci. Pol. Chem.* **2010**, *48*, 1374-1382.

[14] H. C. Aspinall, S. R. Moore, A. K. Smith, J. Chem. Soc.-Dalton Trans.; *J. Chem. Soc. Dalton Trans.* **1993**, 993-996.

[15] O. Tardif, Z. M. Hou, M. Nishiura, T. Koizumi, Y. Wakatsuki, *Organometallics* **2001**, *20*, 4565-4573.

[16] O. Tardif, M. Nishiura, Z. M. Hou, *Tetrahedron* **2003**, *59*, 10525-10539.

[17] K. Izod, S. T. Liddle, W. Clegg, *Chem. Commun.* **2004**, 1748-1749.

[18] V. D. Bianco, S. Doronzo, *Inorg. Synth.* **1976**, *16*, 161.

[19] J. S. Ritch, D. Julienne, S. R. Rybchinski, K. S. Brockman, K. R. D. Johnson, P. G. Hayes, *Dalton Trans.* **2014**, *43*, 267-276.

[20] M. S. Winston, J. E. Bercaw, *Organometallics* **2010**, *29*, 6408-6416.

[21] L. Turculet, R. McDonald, *Organometallics* **2007**, *26*, 6821-6826.

[22] K. Izod, J. Stewart, E. R. Clark, W. Clegg, R. W. Harrington, *Inorg. Chem.* **2010**, *49*, 4698-4707.

[23] (a) C. D. Carmichael, M. D. Fryzuk, *Can. J. Chem.* **2010**, *88*, 667-675; (b) Y. N. Chang, L. C. Liang, *Inorg. Chim. Acta* **2007**, *360*, 136-142.

[24] N. R. Andreychuk, D. J. H. Emslie, *Angew. Chem. Int. Ed.* **2013**, *52*, 1696-1699.

[25] (a) D. J. Brauer, H. Burger, G. R. Liewald, *J. Organomet. Chem.* **1986**, *308*, 119-130; (b) M. G. Gardiner, C. L. Raston, *Inorg. Chem.* **1996**, *35*, 4047-4059; (c) J. K. Brask, T. Chivers, G. Schatte, Chem. Commun.; *Chem. Commun.* **2000**, 1805-1806; (d) S. Daniele, C. Drost, B. Gehrhus, S. M. Hawkins, P. B. Hitchcock, M. F. Lappert, P. G. Merle, S. G. Bott, *J. Chem. Soc. Dalton Trans.* **2001**, 3179-3188; (e) E. Gellermann, U. Klingebiel, T. Pape, F. D. Antonia, T. R. Schneider, S. Schmatz, *Z. Anorg. Allg. Chem.* **2001**, *627*, 2581-2588; (f) J. F. Li, L. H. Weng, X. H. Wei, D. S. Liu, *J. Chem. Soc. Dalton Trans.* **2002**, 1401-1405; (g) T. Chivers, C. Fedorchuk, G. Schatte, J. K. Brask, *Can. J. Chem.* **2002**, *80*, 821-831; (h) J. S. Hao, X. H. Wei, S. P. Huang, J. P. Guo, D. S. Liu, *Appl. Organomet. Chem.* **2005**, *19*, 1010-1014; (i) J. S. M. Lehn, S. Javed, D. M. Hoffman, *Inorg. Chem.* **2007**, *46*, 993-1000; (j) A. M. Corrente, T. Chivers, *Inorg. Chem.* **2008**, *47*, 10073-10080.

[26] M. Driess, G. Huttner, N. Knopf, H. Pritzkow, L. Zsolnai, *Angew. Chem. Int. Ed. Engl.* **1995**, *34*, 316-318.

[27] G. W. Rabe, S. Kheradmandan, G. P. A. Yap, *Inorg. Chem.* **1998**, *37*, 6541-6543.

[28] K. F. Tesh, B. D. Jones, T. P. Hanusa, J. C. Huffman, *J. Am. Chem. Soc.* **1992**, *114*, 6590-6591.

[29] M. Westerhausen, S. Weinrich, B. Schmid, S. Schneiderbauer, M. Suter, H. Noth, H. Piotrowski, *Z. Anorg. Allg. Chem.* **2003**, *629*, 625-633.

[30] (a) C. N. Smit, T. A. Vanderknaap, F. Bickelhaupt, *Tetrahedron Lett.* **1983**, *24*, 2031-2034; (b) L. Weber, D. Bungardt, R. Boese, D. Bläser, *Chem. Ber.-Recl.* **1988**, *121*, 1033-1038.

[31] C. Frenzel, E. Hey-Hawkins, *Phosphorus Sulfur Silicon Relat. Elem.* **1998**, *143*, 1-17.

[32] N. Tokitoh, A. Tsurusaki, T. Sasamori, *Phosphorus Sulfur Silicon Relat. Elem.* **2009**, *184*, 979-986.

[33] M. Westerhausen, S. Schniederbauer, M. Hartmann, M. Warchhold, H. Noth, *Z. Anorg. Allg. Chem.* **2002**, *628*, 330-332.

[34] Y. D. Lv, X. Xu, Y. F. Chen, X. B. Leng, M. V. Borzov, *Angew. Chem. Int. Ed.* **2011**, *50*, 11227-11229.

[35] W. Y. Yi, J. Zhang, L. C. Hong, Z. X. Chen, X. G. Zhou, *Organometallics* **2011**, *30*, 5809-5814.

[36] S. T. Liddle, P. L. Arnold, *Dalton Trans.* **2007**, 3305-3313.

[37] M. R. Crimmin, A. J. P. White, *Chem. Commun.* **2012**, *48*, 1745-1747.

[38] S. Krieck, H. Gorls, M. Westerhausen, *Inorg. Chem. Commun.* **2009**, *12*, 409-411.

[39] M. Westerhausen, M. Hartmann, W. Schwarz, Inorg. Chim. Acta; *Inorg. Chim. Acta* **1998**, *269*, 91-100.

[40] Burger, B. J.; Bercaw J. E. *Vacuum Line Techniques for Handling Air-Sensitive Organometallic Compounds*. In *Experimental Organometallic Chemistry: A Practicum in Synthesis and Characterization*; Wayda, A. L., Darensbourg, M. Y., Eds.; ACS Symp. Ser.; American Chemical Society: Washington D.C., 1987, Vol. 357, pp 79-98.

[41] J. S. Nowick, P. Ballester, F. Ebmeyer, J. Julius Rebek, *J. Am. Chem. Soc.* **1990**, *112*, 8902-8906.

[42] F. Estler, G. Eickerling, E. Herdtweck, R. Anwander, *Organometallics* **2003**, *22*, 1212-1222.

[43] (a) V. Chandrasekhar, P. Sasikumar, R. Boomishankar, G. Anantharamian, *Inorg. Chem.* **2006**, *45*, 3344-3351; (b) G. M. Whitesides, M. Eisenhut, W. M. Bunting, *J. Am. Chem. Soc.* **1974**, *96*, 5398.

[44] E. M. Matson, W. P. Forrest, P. E. Fanwick, S. C. Bart, *Organometallics* **2012**, *31*, 4467-4473.

Entry for the Table of Contents

Layout 2:

FULL PAPER

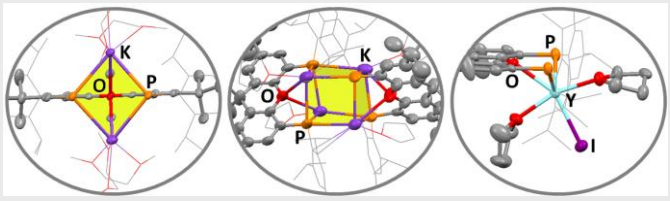

A rigid bis-phosphido POP-donor ligand was synthesized and complexed with potassium and yttrium. This yielded a unique example of a cubic $K_4(PR_2)_4$ cage and a bonding mode to yttrium that differs significantly from that of the bis-amido analogue.

Phosphido Complexes

Kelly S. A. Motolko, David J. H. Emslie, Hilary A. Jenkins and James F. Britten*

Page No. – Page No.

Potassium and Yttrium Complexes of a Rigid Bis-Phosphido POP-Donor Ligand